Thermodynamical Limit of the Lipkin-Meshkov-Glick Model

Pedro Ribeiro, Julien Vidal, and Rémy Mosseri

Laboratoire de Physique Théorique de la Matière Condensée, CNRS UMR 7600, Université Pierre et Marie Curie, 4 Place Jussieu, 75252 Paris Cedex 05, France

(Received 19 March 2007; published 2 August 2007)

A method based on the analysis of the Majorana polynomial roots is introduced to compute the spectrum of the Lipkin-Meshkov-Glick model in the thermodynamical limit. A rich structure made of four qualitatively different regions is revealed in the parameter space, whereas the ground state study distinguishes between only two phases.

DOI: 10.1103/PhysRevLett.99.050402 PACS numbers: 05.30.−d, 03.65.Sq, 21.60.Ev

The Lipkin-Meshkov-Glick (LMG) model introduced in 1965 to describe the shape phase transition in nuclei [1] has, since then, been proposed to describe many systems ranging from interacting spin systems [2] to Bose-Einstein condensates [3] or magnetic molecules such as Mn_{12} acetate [4]. This ubiquity is due to its mapping onto a single particle evolving in a double-well potential [5,6] or onto an interacting two-level boson system. More recently, this model has also been used to investigate the relationship between entanglement and quantum phase transitions [7–10].

The LMG model is known to be exactly solvable [11–13]. However, getting the solution requires solving Bethe-like equations, a task which, in the present context, is more costly than exact diagonalization. A complete description of the spectrum thus requires developing alternative routes. Though the low-energy spectrum has been studied in detail via different methods (variational [1], bosonization [9,14], coherent states [15]), the richness of the full spectrum has been investigated only lately by means of numerical diagonalizations [16,17]. These latter studies suggest the existence of singular points in the density of states as well as a nontrivial level spacing distribution.

In this Letter, we shed light on these issues by exactly computing the spectrum of the LMG model. The proposed method relies on the determination of the Majorana polynomial roots associated with the eigenstates of the Hamiltonian. This polynomial is built within a coherent state formalism which is well suited to such a system. Within this framework, the spectrum is encoded in a linear differential equation which is solved in the thermodynamical limit. This allows us to exactly compute the density of states in the whole parameter range and to locate its singularities. Four distinct regions arise with qualitatively different properties. In particular, we find a parameter regime for which the density of states has no thermodynamical limit.

The LMG model describes a set of N spin-$\frac{1}{2}$ mutually interacting through a XY-like Hamiltonian and coupled to an external transverse magnetic field h. This Hamiltonian H can thus be expressed in terms of the total spin operators $S_\alpha = \sum_{i=1}^{N} \sigma_\alpha^i/2$, where the σ_α's are the Pauli matrices:

$$H = -\frac{1}{N}(\gamma_x S_x^2 + \gamma_y S_y^2) - hS_z. \tag{1}$$

In the following, we consider only the maximum spin sector $s = N/2$, with N even. Given the symmetry of the spectrum of H, we focus on the parameter range $h \geq 0$; $0 \leq |\gamma_y| \leq \gamma_x$. Note also that $[H, \mathbf{S}^2] = 0$ and $[H, e^{i\pi(S_z - s)}] = 0$ (spin-flip symmetry). Denoting by $\{|s, m\rangle\}$ the standard eigenbasis of $\{\mathbf{S}^2, S_z\}$, this latter symmetry implies that odd and even states decouple. In the thermodynamical limit, both subspaces are isospectral, so we limit the following analysis to the sector m even for which one has exactly $(s + 1)$ eigenstates.

In the spin coherent states basis [18], with non-normalized states $|\alpha\rangle = e^{\bar{\alpha} S_+}|s, -s\rangle$, any state $|\Psi\rangle$ is represented by its Majorana polynomial [19] defined as

$$\Psi(\alpha) = \langle \alpha|\Psi\rangle = \sum_{m=-s}^{s} \sqrt{\frac{(2s)!}{(s-m)!(m+s)!}} \langle s, m|\Psi\rangle \alpha^{m+s} = C \prod_{k=1}^{d} (\alpha - \alpha_k), \tag{2}$$

where $d \leq 2s$ is its degree.

The standard representation of the spin operators ($S_\pm = S_x \pm iS_y$) in the coherent states basis

$$S_+ = 2s\alpha - \alpha^2 \partial_\alpha, \tag{3}$$

$$S_- = \partial_\alpha, \tag{4}$$

$$S_z = -s + \alpha \partial_\alpha \tag{5}$$

allows one to map the Schrödinger equation $H|\Psi\rangle = E|\Psi\rangle$ onto the following linear differential equation [5,20]:

$$\left[\frac{P_2(\alpha)}{(2s)^2}\partial_\alpha^2 + \frac{P_1(\alpha)}{2s}\partial_\alpha + P_0(\alpha)\right]\Psi(\alpha) = \varepsilon \Psi(\alpha), \tag{6}$$

where $\varepsilon = E/s$ and

$$P_0(\alpha) = \frac{1}{4s}[\alpha^2(2s-1)(\gamma_y - \gamma_x) - \gamma_x - \gamma_y] + h, \tag{7}$$

$$P_1(\alpha) = \alpha\left\{\frac{2s-1}{2s}[\alpha^2(\gamma_x - \gamma_y) - \gamma_x - \gamma_y] - 2h\right\}, \tag{8}$$

$$P_2(\alpha) = -\frac{1}{2}[(\alpha^2-1)^2\gamma_x - (\alpha^2+1)^2\gamma_y]. \quad (9)$$

Except for trivial values of the parameters, the degree of Ψ for an eigenstate of H in the sector we considered is $d = 2s$. At this step, the spectrum could be analyzed by mapping Eq. (6) onto a Schrödinger equation describing a particle in an effective one-dimensional potential [5,6]. Then a semiclassical treatment would, in principle, allow one to obtain the density of states in the thermodynamical limit, as shown in Ref. [4] for the low-energy spectrum in the region $\gamma_y = 0$, $\gamma_x > 0$. Unfortunately, for arbitrary values of the parameters, the effective potential becomes tricky [6], and such an approach is therefore difficult to follow. Here we propose an alternative route by first converting the linear second-order differential equation for Ψ (6) into a first-order differential equation for its logarithmic derivative. More precisely, the function G defined as

$$G(\alpha) = \frac{1}{2s}\partial_\alpha \log\Psi(\alpha) = \frac{1}{2s}\sum_{k=1}^{2s}\frac{1}{\alpha-\alpha_k} \quad (10)$$

satisfies the following Riccati-like equation:

$$P_2(\alpha)\left[\frac{G'(\alpha)}{2s} + G^2(\alpha)\right] + P_1(\alpha)G(\alpha) + P_0(\alpha) = \varepsilon. \quad (11)$$

The density of states is then given by analyzing the poles of G, i.e., the roots of the Majorana polynomial Ψ. Indeed, the cornerstone of this study is that, for this model, the α_k's are spread over two curves $\mathcal{C}_0$ and $\mathcal{C}_1$ in the complex plane which depend on the energy. In addition, the nth excited state of H has $2n$ poles on $\mathcal{C}_1$ and $2(s-n)$ on $\mathcal{C}_0$ (thus defining both curves). This remarkable property stems from the oscillation theorem which indexes the excited states for a particle in the effective one-dimensional potential (discussed above) by the number of wave function nodes. To illustrate this repartition of the poles which is likely related to the integrability of the model [21], we display in Fig. 1 several typical states in the Majorana sphere representation [19]. This representation generalizes the celebrated Bloch sphere used for spin-$\frac{1}{2}$ states and proceeds as follows. For a given polynomial with d roots, we first complement it with $(2s-d)$ roots at infinity in the complex plane. Next, the resulting set of $2s$ points is sent onto the unit sphere by an inverse stereographic map. For instance, within this mapping, the basis state $|s,m\rangle$ is represented by $(s-m)$ points on one pole and $(s+m)$ points on the opposite pole.

The location of the poles of G explained above provides a straightforward relation between the normalized integrated density of states $\mathcal{N} \in [0,1]$ and the number of poles lying in $\mathcal{C}_1$. One indeed simply has

$$\mathcal{N}(\varepsilon) = \frac{n+1}{s+1} = \frac{1}{s+1}\left[\frac{s}{2i\pi}\oint_{\tilde{\mathcal{C}}_1} G(\alpha)d\alpha + 1\right], \quad (12)$$

where $\tilde{\mathcal{C}}_1$ is a contour that surrounds $\mathcal{C}_1$ and oriented such that $\mathcal{N} \geq 0$. In this equation, G is built from the nth excited state, and the dependence of $\mathcal{N}$ with ε is given

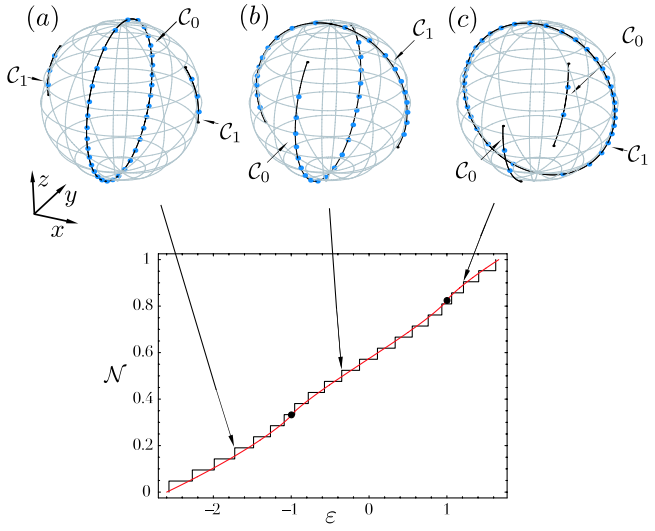

FIG. 1 (color online). Upper part: Representation of the poles of G on the Majorana sphere (blue dots) for three typical eigenstates computed for $h = 1$, $\gamma_x = 5$, $\gamma_y = -3$, and $s = 20$ (zone III in Fig. 2). Black lines correspond to the G_0 branch cuts $\mathcal{C}_0$ and $\mathcal{C}_1$. Lower part: Numerical (black staircase curve $s = 20$) versus analytical (red line $s = \infty$) integrated density of states. Black dots indicates the singularity of the density of states $N_0^{\mathrm{III}}(-h)$ and $N_0^{\mathrm{III}}(h)$ [Eqs. (18) and (21), respectively] in the thermodynamical limit.

via Eq. (11). Unfortunately, one cannot solve Eq. (11) exactly at finite s, which would give a complete explicit solution to our problem. However, one can easily solve it perturbatively in $1/s$.

Therefore, let us assume that G, and ε, can be expanded in the following form:

$$G = \sum_{i\in\mathbb{N}}\frac{G_i}{s^i}, \qquad \varepsilon = \sum_{i\in\mathbb{N}}\frac{\varepsilon_i}{s^i}. \quad (13)$$

At leading order s^0, Eq. (11) becomes a second-order polynomial equation for G_0 whose solutions simply read

$$G_0^{\pm}(\alpha) = \frac{\alpha[\alpha^2(\gamma_y-\gamma_x)+\gamma_x+\gamma_y+2h] \pm \sqrt{2Q(\alpha)}}{2P_2(\alpha)}, \quad (14)$$

where

$$Q(\alpha) = (\gamma_y-\gamma_x)(h+\varepsilon_0)\alpha^4 + 2[h^2+\gamma_x\gamma_y+\varepsilon_0(\gamma_x+\gamma_y)]\alpha^2 + (\gamma_x-\gamma_y)(h-\varepsilon_0). \quad (15)$$

The four roots of Q are the branch points of G which define the limit of the curves $\mathcal{C}_0$ and $\mathcal{C}_1$. A close analysis of these branch cuts, in the parameter space, then leads to the integrated density of states in the thermodynamical limit, which reads

$$\lim_{s\to\infty}\mathcal{N}(\varepsilon)=\mathcal{N}_0(\varepsilon_0)=\frac{1}{2i\pi}\int_{\mathcal{C}_1}[G_0^+(\alpha)-G_0^-(\alpha)]d\alpha. \tag{16}$$

This quantity can be expressed in terms of lengthy expressions involving elliptic integrals. We obtained these expressions in the whole parameter space and will give them explicitly in a forthcoming publication [22]. In the following, we discuss only qualitatively the various regions that must be distinguished and analyze them by means of the density of states $\rho_0(\epsilon_0)=\partial_{\varepsilon_0}\mathcal{N}_0(\varepsilon_0)$.

But, first of all, let us remind the reader that if one considers only the properties of the ground state, which define the zero-temperature phase diagram, only two phases must be distinguished. For $h>\gamma_x$ (symmetric phase), the ground state is unique and $\lim_{s\to\infty}\langle S_z\rangle/s=1$, whereas for $h<\gamma_x$ (broken phase), the ground state is twofold degenerate and $\lim_{s\to\infty}\langle S_z\rangle/s=h/\gamma_x$. The quantum phase transition at $h=\gamma_x$ is second-order and characterized by mean-field critical exponents [2] and nontrivial finite-size scaling behavior [9,23]. An important result of our study is that, when considering the full spectrum, four different zones arise instead of two. These regions, described below, are characterized by different singular behaviors of the density of states (see Fig. 2) as already noticed in a numerical study of the special case $\gamma_x=-\gamma_y$ [16].

Zone I: $|\gamma_y|<\gamma_x<h$.—In this sector, the density of states ρ_0 is a smooth function of $-h\le\varepsilon_0\le h$ as can be seen in Fig. 2. The distribution of Majorana polynomial roots for the eigenstates is similar to that displayed in Fig. 1(b). In the complex plane, $\mathcal{C}_0$ and $\mathcal{C}_1$ lie in the imaginary and real axes, respectively.

Zone II: $|\gamma_y|<h<\gamma_x$.—In this region, two distinct branches must be distinguished: II(a) $-[(h^2+\gamma_x^2)/2\gamma_x]\le\varepsilon_0\le-h$. $\mathcal{C}_0$ coincides with the whole imaginary axis, while $\mathcal{C}_1$ is made of two disconnected segments in the real axis as depicted in Fig. 1(a). II(b) $-h\le\varepsilon_0\le h$. $\mathcal{C}_0$ and $\mathcal{C}_1$ are the same as in I.

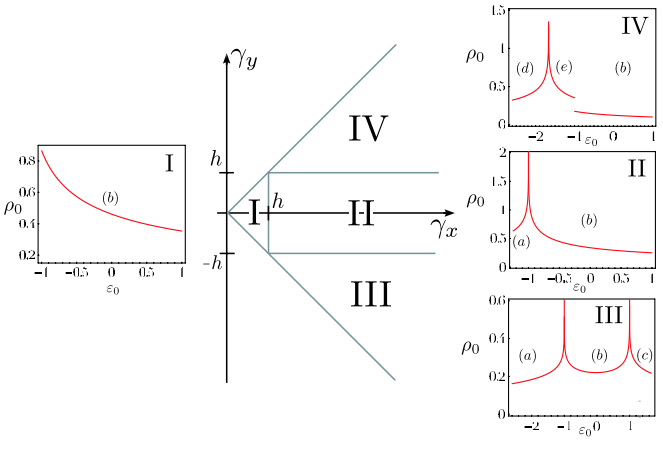

FIG. 2 (color online). Phase diagram in the γ_x, γ_y plane at fixed $h>0$ and typical density of states for (γ_x, γ_y, h) equal to I: (1/2, 1/3, 1), II: (2, 1/2, 1), III: (5, −3, 1), and IV: (5, 3, 1).

These two branches of the density of states diverge at $\varepsilon_0=-h$, where the elliptic integrals involved in the expression of $\mathcal{N}_0$ can be recasted in the simple following form:

$$\mathcal{N}_0^{\mathrm{II}}(-h)=1-\frac{2}{\pi\sqrt{\gamma_x\gamma_y}}\times\left[A_h^+\tan^{-1}\frac{A_h^+}{B_h^0}-A_h^-\tan^{-1}\frac{A_h^-}{B_h^+}\right], \tag{17}$$

with

$$A_h^\pm=h\pm\sqrt{\gamma_x\gamma_y}, \tag{18}$$

$$B_h^0=\sqrt{h\gamma_x}+\sqrt{h\gamma_y}+\sqrt{(\gamma_x-h)(h-\gamma_y)}, \tag{19}$$

$$B_h^\pm=\pm(\sqrt{h\gamma_x}-\sqrt{h\gamma_y})+\sqrt{(\gamma_x-h)(h-\gamma_y)}. \tag{20}$$

Zone III: $h<-\gamma_y<\gamma_x$.—In this zone, there are three different branches: III(a) $-[(h^2+\gamma_x^2)/2\gamma_x]\le\varepsilon_0\le-h$. $\mathcal{C}_0$ and $\mathcal{C}_1$ are the same as in II(a). III(b) $-h\le\varepsilon_0\le h$. $\mathcal{C}_0$ and $\mathcal{C}_1$ are the same as in I. III(c) $h\le\varepsilon_0\le-[(h^2+\gamma_y^2)/2\gamma_y]$. $\mathcal{C}_0$ is made of two disconnected segments in the imaginary axis, while $\mathcal{C}_1$ coincides with the whole real axis as depicted on the Majorana sphere in Fig. 1(c).

In this zone, the density of states has two singularities at $\varepsilon_0=\pm h$. Their position in the spectrum is given by $\mathcal{N}_0^{\mathrm{III}}(-h)=\mathcal{N}_0^{\mathrm{II}}(-h)$ [see Eq. (18)] and

$$\mathcal{N}_0^{\mathrm{III}}(h)=\frac{2}{\pi\sqrt{\gamma_x\gamma_y}}\left[A_h^+\tan^{-1}\frac{A_h^+}{B_{-h}^0}-A_h^-\tan^{-1}\frac{A_h^-}{B_{-h}^-}\right]. \tag{21}$$

For $\gamma_x=-\gamma_y$, the density of states is symmetric with respect to $\varepsilon_0=0$, and the above expression gives the exact location, in the thermodynamical limit, of the so-called exceptional point observed in Ref. [16].

Zone IV: $h<\gamma_y<\gamma_x$.—This part of the phase diagram is the most complex one. The density of states is, as in zone III, made of three different branches: IV(d) $-[(h^2+\gamma_x^2)/2\gamma_x]\le\varepsilon_0\le-[(h^2+\gamma_y^2)/2\gamma_y]$; IV(e) $-[(h^2+\gamma_y^2)/2\gamma_y]\le\varepsilon_0\le-h$; IV(b) $-h\le\varepsilon_0\le h$.

However, the structure of the $\mathcal{C}_1$ curve, in each case, is complex, but $\mathcal{C}_0$ remains simple so that the integral in Eq. (16) can still be computed and reveals two special points. The first one occurs at $\varepsilon_0=-[(h^2+\gamma_y^2)/2\gamma_y]$, for which

$$\mathcal{N}_0^{\mathrm{IV}}\left(-\frac{h^2+\gamma_y^2}{2\gamma_y}\right)=1-\frac{1}{\pi\sqrt{\gamma_x\gamma_y}}\times[A^+\tan^{-1}C_h-A^-\tan^{-1}C_{-h}], \tag{22}$$

with

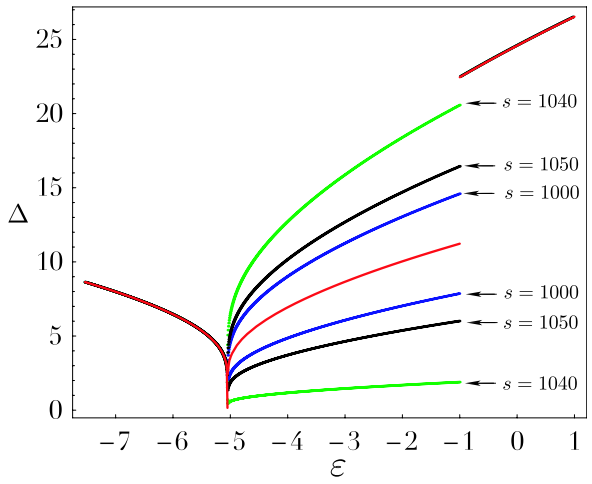

FIG. 3 (color online). Gap between two consecutive levels as a function of the energy in region IV for $\gamma_x = 15$, $\gamma_y = 10$, and $h = 1$. In the central region, the middle red line is the average gap Δ_0 in the thermodynamical limit. The branches below and above this line are, respectively, $\Delta^{(-)}$ and $\Delta^{(+)}$ (see text).

$$C_h = \frac{h\sqrt{\gamma_x} + \gamma_y^{3/2}}{\sqrt{(\gamma_x - \gamma_y)(\gamma_y^2 - h^2)}}. \tag{23}$$

There, the density of states diverges as in zones II and III. The second one arises at $\varepsilon_0 = -h$, where

$$\mathcal{N}_0^{\mathrm{IV}}(-h) = 1 - \frac{h}{\sqrt{\gamma_x \gamma_y}}, \tag{24}$$

but, at this energy, *the density of states is discontinuous in the thermodynamical limit* as can be seen in Fig. 2.

We have confirmed this anomalous behavior numerically and observed an even more surprising result. Indeed, the energy difference between two consecutive levels $\Delta^{(i)} = E^{(i+1)} - E^{(i)}$ $(i = 1, \ldots, s)$ is normally given by $\Delta_0(\varepsilon_0) = 1/\rho_0(\varepsilon_0)$ in the thermodynamic limit. However, in region IV(e), numerical results (at finite s) show that it is not the case. Instead, $\Delta^{(i)}$ spreads over two branches $(+)$ and $(-)$, depending on the parity of the i. In addition, these branches oscillate without converging when s increases as can be seen in Fig. 3. In this case, the gap we computed, in the thermodynamical limit, is the average gap, namely, $\Delta_0(\varepsilon_0) = \frac{1}{2}[\Delta^{(+)}(\varepsilon_0) + \Delta^{(-)}(\varepsilon_0)]$.

To understand physically this unusual phenomenon, we have analyzed the classical trajectories in this region and have observed that there are two possible classical trajectories [22]. Using the results described in Ref. [20], we computed analytically the expectation values of several observables (such as the magnetization) as a function of energy. We found that these values also depend on the parity of the level considered, but, contrary to the gap, the two branches converge in the thermodynamical limit.

Finally, note that, for $h = 0$, the LMG model in this region coincides with the quantum asymmetric rotor model [24].

In conclusion, we emphasize that the present approach can be extended to other similar models with higher-order interaction terms where the mapping onto a particle in a one-dimensional potential fails. Further, one can go beyond the thermodynamical limit and extract the finite-s corrections which could be crucial for some observables [22].

We are grateful to C. Aslangul, S. Dusuel, N. Gromov, J.-M. Maillard, and P. Vieira for fruitful and stimulating discussions. P. R. was partially supported by FCT and EU FEDER through POCTI and POCI, namely, via QuantLog No. POCI/MAT/55796/2004 Project of CLC-DM-IST, SQIG-IT, and Grant No. SFRH/BD/16182/2004/2ZB5.

[1] H. J. Lipkin, N. Meshkov, and A. J. Glick, Nucl. Phys. **62**, 188 (1965).
[2] R. Botet and R. Jullien, Phys. Rev. B **28**, 3955 (1983).
[3] J. I. Cirac, M. Lewenstein, K. Mølmer, and P. Zoller, Phys. Rev. A **57**, 1208 (1998).
[4] D. A. Garanin, X. Martínez Hidalgo, and E. M. Chudnovsky, Phys. Rev. B **57**, 13 639 (1998).
[5] A. V. Turbiner, Commun. Math. Phys. **118**, 467 (1988).
[6] V. V. Ulyanov and O. B. Zaslavskii, Phys. Rep. **216**, 179 (1992).
[7] J. Vidal, G. Palacios, and R. Mosseri, Phys. Rev. A **69**, 022107 (2004).
[8] J. I. Latorre, R. Orús, E. Rico, and J. Vidal, Phys. Rev. A **71**, 064101 (2005).
[9] S. Dusuel and J. Vidal, Phys. Rev. Lett. **93**, 237204 (2004).
[10] T. Barthel, S. Dusuel, and J. Vidal, Phys. Rev. Lett. **97**, 220402 (2006).
[11] F. Pan and J. P. Draayer, Phys. Lett. B **451**, 1 (1999).
[12] J. Links, H.-Q. Zhou, R. H. McKenzie, and M. D. Gould, J. Phys. A **36**, R63 (2003).
[13] G. Ortiz, R. Somma, J. Dukelsky, and S. Rombouts, Nucl. Phys. **B707**, 421 (2005).
[14] A. Dzhioev, Z. Aouissat, A. Storozhenko, A. Vdovin, and J. Wambach, Phys. Rev. C **69**, 014318 (2004).
[15] A. Kuriyama *et al.*, J. Phys. A **36**, 10 361 (2003).
[16] W. D. Heiss, F. G. Scholz, and H. B. Geyer, J. Phys. A **38**, 1843 (2005).
[17] O. Castaños, R. López-Peña, J. G. Hirsch, and E. López-Moreno, Phys. Rev. B **74**, 104118 (2006).
[18] J. R. Klauder and B. S. Skagerstam, *Coherent States* (World Scientific, Singapore, 1985).
[19] E. Majorana, Nuovo Cimento **9**, 43 (1932).
[20] J. Kurchan, P. Leboeuf, and M. Saraceno, Phys. Rev. A **40**, 6800 (1989).
[21] P. Leboeuf and A. Voros, J. Phys. A **23**, 1765 (1990).
[22] P. Ribeiro, J. Vidal, and R. Mosseri (to be published).
[23] F. Leyvraz and W. D. Heiss, Phys. Rev. Lett. **95**, 050402 (2005).
[24] G. W. King, J. Chem. Phys. **15**, 820 (1947).